

FADE: A Dataset for Detecting Falling Objects around Buildings in Video

Zhigang Tu, *Senior Member, IEEE*, Zitao Gao, Zhengbo Zhang, Chunlun Zhou,
Junsong Yuan, *Fellow, IEEE*, Bo Du, *Senior Member, IEEE*

Abstract—Falling objects from buildings can cause severe injuries to pedestrians due to the great impact force they exert. Although surveillance cameras are installed around some buildings, it is challenging for humans to capture such events in surveillance videos due to the small size and fast motion of falling objects, as well as the complex background. Therefore, it is necessary to develop methods to automatically detect falling objects around buildings in surveillance videos. To facilitate the investigation of falling object detection, we propose a large, diverse video dataset called FADE (Falling Object DETection around Buildings) for the first time. FADE contains 1,881 videos from 18 scenes, featuring 8 falling object categories, 4 weather conditions, and 4 video resolutions. Additionally, we develop a new object detection method called FADE-Net, which effectively leverages motion information and produces small-sized but high-quality proposals for detecting falling objects around buildings. Importantly, our method is extensively evaluated and analyzed by comparing it with the previous approaches used for generic object detection, video object detection, and moving object detection on the FADE dataset. Experimental results show that the proposed FADE-Net significantly outperforms other methods, providing an effective baseline for future research. The dataset and code are publicly available at <https://fadedataset.github.io/FADE.github.io/>.

Index Terms—Falling object detection, a large diverse video dataset, baseline method.

I. INTRODUCTION

OVER the past few decades, with the continuous expansion of urbanization, high-rise buildings have sprung up. Some people, who throw objects from tall buildings arbitrarily, causing injuries and incidents one after another. According to a report [1] of the U.S. Bureau of Labor Statistics, there are more than 50,000 “struck by falling objects” injuries every year in USA. We use a specific example to illustrate the possible hazards of objects falling from tall buildings. If a 200-gram apple drops from a 30-meter building, the impact duration of the apple is approximate 0.01 seconds. Based on the momentum theorem [2], it means that the ground will bear an impact of about 49.5-kilogram weight. As depicted in Figure 1, this type of incident profoundly endangers public safety. To reduce such incidents, some countries have legislated to rule



Fig. 1. The incident of falling object around the building produces great danger and harm to human life and social security.

that throwing objects from buildings is illegal, e.g., USA [3], Singapore [4], China [5], etc. With more and more cameras installed around buildings, it is *necessary* to explore how to effectively detect these falling object events by utilizing the surveillance videos.

Intelligent video surveillance (IVS) has become a crucial technology for public safety [6]. Recent advances in computer vision promoted the development of IVS systems for various security applications, including object detection [7]–[9], anomaly detection [10]–[13], human identification [14]–[16], tracking [17]–[19], and behavior understanding [20]–[23]. These computer vision based methods have advantages of low cost, high precision, and manpower saving. Inspired by the successful applications of these computer vision techniques, some research institutions and government departments have begun to explore computer vision algorithms for detecting the incidents of falling objects around buildings. The task of falling object detection around buildings (FODB) can be considered as a special case of moving object detection (MOD). Although there have been several MOD datasets, such as SABS [24], CDnet 2014 [25], GTFD [26], and LASIESTA [27], the objects of interest in these datasets differ from those in FODB largely. The falling objects in FODB are usually much smaller and move faster, making them more difficult to detect.

A comparison between the FODB task and the MOD task is shown in Figure 2. Where in an existing MOD dataset, the moving object occupies a large area of the image. In contrast,

Corresponding authors: Zitao Gao, Zhengbo Zhang (Email: gaozitao@whu.edu.cn, zhengbozhang.1@gmail.com).

Zhigang Tu, Zitao Gao, and Zhengbo Zhang are with the State Key Laboratory of Information Engineering in Surveying, Mapping and Remote Sensing, Wuhan University, Wuhan 430079, China.

Chunlun Zhou is with Ant Group co Ltd, Beijing 100020, China.

Junsong Yuan is with the Computer Science and Engineering Department, The State University of New York at Buffalo, Buffalo, NY 14260 USA.

Bo Du is with the School of Computer Science, Wuhan University, Wuhan 430072, China.

FODB task

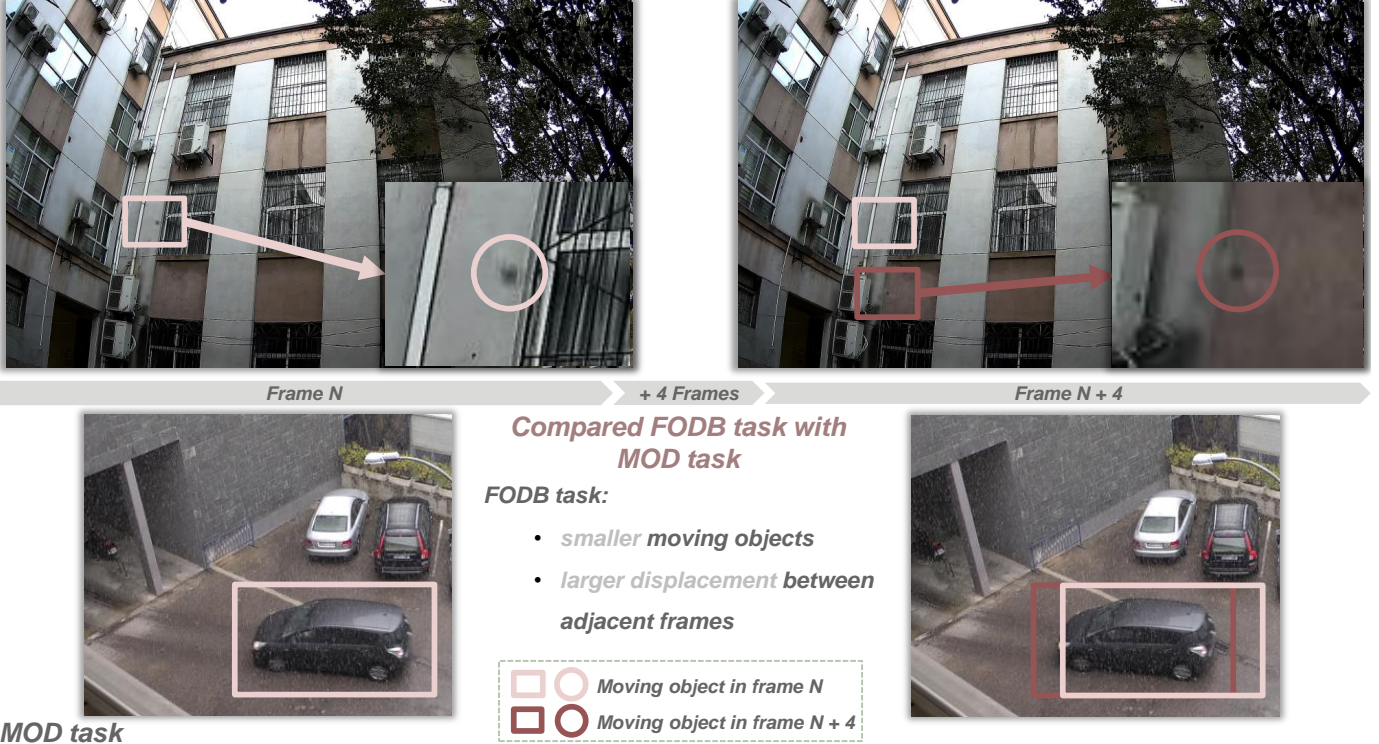


Fig. 2. Comparison the tasks of FODB and MOD. By observing four frames (two frames above are from our dataset, and two frames below are from the LASIESTA dataset [27]) from two video sequences, we can find that the moving object in FODB task is much smaller and has larger displacement between successive frames. To see the falling object in the FODB task clearly, we enlarge the object and place it in the lower right corner of the video frame.

the falling object from the building takes up a small area of the image, causing it is difficult to distinguish the falling objects from the background. Generally, the motion of the falling object in the FODB task is fast, resulting in 1) motion blur and 2) a large displacement of the object between adjacent video frames, which are uncommon in the MOD dataset. Furthermore, none of the existing MOD datasets cover the categories of falling objects around buildings. Consequently, it is *necessary* to collect a large diverse dataset as well as propose an effective baseline method for FODB. Such efforts are crucial for advancing the progress and practical application of FODB.

In this work, for the first time, we present a completely new video dataset termed FADE for FODB, which consists of 1,881 videos under various scenes. Specifically, the dataset contains 164,314 video frames in total, all of which are annotated. Our dataset is diverse, covering 18 scenes, 8 object categories, 4 video resolutions, 4 weather conditions, 3 camera angles, and 2 lighting conditions. As can be seen in Table I, our dataset FADE has richer data compared to the existing MOD datasets. The size of the falling object in our FADE is small (shown in Table II) with a median area of about 20 pixels, which is much smaller than the small object ($area < 32^2$ pixels) defined in the COCO dataset [28]. We also propose a new baseline method, FADE-Net, which utilizes motion cues to complement appearance features and modifies the region proposal network to generate high-quality proposals for small falling objects.

We use the evaluation metrics in the MOD task to bench-

mark several methods of 3 different tasks (MOD, generic object detection, and video object detection) on our dataset. We also explore a new metric, time range overlap (TRO), to evaluate the performance of the detection methods on localizing the object falling incidents. The experimental results indicate that FODB is a challenging task and validate the effectiveness of our presented method.

The main contributions of our work are three-fold:

- We construct a new video dataset called FADE which is the first dataset used for falling object detection around buildings (FODB). This dataset is large and diverse, which covers various scenes and complex conditions.
- We explore a new baseline method FADE-Net for the FODB task, which effectively utilizes motion cues and generates high-quality proposals for small-sized falling objects detection.
- We evaluate the proposed FADE-Net, and other methods, *i.e.* MOD methods, generic object detection methods and video object detection methods, on our FADE dataset comprehensively, which can be served as a benchmark for future research on FODB.

II. RELATED WORK

Moving Object Detection Dataset. MOD is a basic task in computer vision, and some MOD datasets have been released for training and testing the MOD algorithms. Early MOD datasets, e.g. Wallflower [29], SegTrack [30], and I2R [31], are small in scale. Wallflower [29] is one of the earliest

TABLE I

COMPARISON OF OUR FADE DATASET WITH THE PRIOR MOD DATASETS. “GT FRAMES” MEANS THE GROUND TRUTH FRAMES. THE DATASETS ARE SORTED BY THE PUBLISHING TIME IN ASCENDING ORDER. THE MAXIMUM QUANTITY AND THE SECOND MAXIMUM QUANTITY ARE HIGHLIGHTED IN **BOLD** AND UNDERLINE, RESPECTIVELY. OUR FADE DATASET HAS THE LARGEST NUMBER OF VIDEOS, TOTAL FRAMES, GT FRAMES, AND SCENES.

Dataset	Total videos \uparrow	Total frames	GT frames	Scenes
SABS [24]	9	6,408	2,000	9
SegTrack V2 [33]	14	976	976	14
SBI [37]	14	5,024	14	14
GTFD [26]	25	1,067	1,067	7
CDnet 2014 [25]	31	<u>90,000</u>	<u>90,000</u>	11
LASIESTA [27]	48	18,425	18,425	4
DAVIS 2016 [36]	<u>50</u>	3,455	3,455	<u>15</u>
FADE (Ours)	1,881	164,314	164,314	18

MOD datasets, which has solely 7 video sequences, and each sequence has only 1 ground truth (GT) frame. SegTrack [30] consists of only 6 video sequences and 215 annotated frames. 10 video sequences are provided in I2R [31], including videos with dynamic backgrounds, challenging weather conditions, and gradual illumination variations. Later, some large scale and complicated MOD datasets are constructed. For instance, SABS [24] contains videos with 10 categories, and each video has 800 training frames. Some testing video frames in FBMS 59 [32] and SegTrack V2 [33] contain multiple moving objects. GTFD [26] provides a collection of 25 videos with both rigid and non-rigid moving objects. LASIESTA [27] consists of 45 videos and 18,425 video frames, recorded by the moving and static cameras. CDnet 2012 [34] and CDnet 2014 [25] are presented as benchmarks in IEEE Change Detection Workshop. CDnet 2014 [25] increases 22 videos and 5 categories on the basis CDnet 2012 [25]. Captured in the outdoor environment, BMC 2012 [35] includes a total of 29 real and synthetic videos in different weather conditions. DAVIS 2016 [36] supplies 50 high-quality and densely annotated videos. SBI [37] composes of 14 image sequences and the corresponding GT backgrounds, which is the first dataset used to evaluate the background initialization approaches.

Unlike these MOD datasets, FADE is the first dataset for FODB which contains numerous videos and diverse scenes. The comparison between our FADE and the prior MOD datasets is shown in Table I.

Moving Object Detection. MOD has been extensively investigated due to its wide range of applications [38]–[40]. Many unsupervised MOD methods have been explored, which can be classified into two categories, *i.e.* background modeling and feature extraction. Specifically, for background modeling, parametric based Gaussian mixture methods [9], [41], [42] are proposed to model the background in MOD. Barnich et al. [8] update the background by applying a novel random selection strategy. Baf et al. [43] apply Choquet integral [44] as an aggregation operator to aggregate color and texture features for MOD. Lin et al. [45] present a dual-rate background modeling framework to detect foreground objects, utilizing both short-term and long-term background models to improve the accuracy of foreground inference. For feature extraction, Yang et al. [46] adopt an optical flow based method to detect moving objects. Zhou et al. [11] use motion information to enhance

detection with motion fusion blocks that compressing video clips into a single image. Thanikasalam et al. [47] exploit a target-specific Siamese attention network that employs residual and channel attention modules to capture the global and channel-wise information of moving objects. Shang et al. [48], [49] consider MOD as a robust principal component analysis problem involving robust subspace learning and tracking [50]–[53]. To address sudden and gradual background changes, Dong et al. [54] explore a clustering feature space method to represent different background appearances. The developments of deep learning [55]–[59] have greatly promoted the progress of supervised MOD methods. Deep learning-based MOD approaches can be divided into six main categories: basic CNN [60]–[64], deep CNN [65], [66], 3D CNN [67], [68], ConvLSTM [69], FCN [70], and GAN [71], [72]. Although numerous MOD methods have been proposed, few can be applied to FODB. We select representative state-of-the-art MOD methods to benchmark our dataset.

Falling Object Detection. There are a few works concentrated on falling object detection. Some use different sensors to handle this task. 3D point cloud of the object generated by the distance sensor, is applied to predict the falling probability of the object in the indoor or at the building site [73]. Alvare et al. [74] utilize the ultrasonic sensor and the signal coding sequence technology, which is based on complementary coding, to detect falling object on railway tracks. By employing the object detection method, Yang et al. [75] obtain the positional relationship between the objects with falling risk and the workers at the building site, and establish an automatic management system for evaluating the falling risk. Different from these methods, our approach utilizes motion cues to complement appearance features for better falling object detection around buildings.

III. THE PROPOSED FADE DATASET

We collect and release the first video dataset for falling object detection around buildings publicly to promote its development. In this section, we introduce our FADE dataset in detail from the aspects of metadata, dataset construction, dataset division and statistics, dataset ethics, license, maintenance plan, and evaluation metrics.



Fig. 3. Four weather conditions in our FODB dataset including fair, cloudy, overcast and rainy.



Fig. 4. We provide videos of two modes (RGB mode and grayscale mode) in various scenes, such as dormitories, classroom buildings, office buildings, etc.

A. Metadata

To provide a comprehensive FODB dataset, we collect videos in diverse weather conditions, lighting cases, scenes, camera angles, and video resolutions. Example video frames are shown in our dataset (<https://fadeddataset.github.io/FADE.github.io/>). Our metadata is defined as follows.

Object Category. To cover classes of the falling objects around buildings as many as possible, we collect 8 category of objects as follows: clothes, shoes, kitchen waste, books, spitballs, bottles, packaging bags, and packaging boxes.

Weather Condition. Different weather conditions lead to different light intensities, which affect the contrast between falling object and the background. Weather condition is one of the most important influences. We design our dataset with 4 weather conditions: fair, cloudy, overcast, and rainy, which can be seen in Figure 3.

Lighting Condition. Generally, when the light intensity is lower than 0.04 Lux, the image of the surveillance video will change from the RGB mode to the grayscale mode. Both the RGB mode and the grayscale mode videos are collected in various scenes to enrich our dataset. As shown in Figure 4, we provide videos in both the RGB mode and the grayscale mode with light intensity more and less than 0.04 Lux, respectively.

Scene. The scene of the falling incident is diverse. Our FADE dataset includes 18 different scenes, covering almost all the scenarios where the falling incidents may occur. E.g.,

classroom buildings, office buildings, dormitories, apartments, and buildings under construction (shown in Figure 4). In our dataset, the scene indicates one viewpoint of a building. In different scenes, the buildings appear different as they are captured in different viewpoints.

Camera Angle. The surveillance cameras for FODB are normally installed 30 meters away from the high-rise buildings, and different floors of the buildings are monitored by cameras from different angles. In our dataset, we consider three different camera angles: 30°, 45°, and 60°.

Video Resolution. Usually, the surveillance video contains a variety of resolutions. To include multifarious data, we provide videos of 4 resolutions: 1280×720 , 1920×1080 , 2560×1440 , and 2592×1520 .

B. Dataset construction

This section introduces how we build our dataset in detail. Our dataset documentation, annotation instruction, intended utilization, and structured metadata are published at the website <https://fadeddataset.github.io/FADE.github.io/index.html>. The example videos and evaluation code are provided in our website. Our data does not contain any personally identifiable information or offensive content. We bear all responsibility in case of violation of rights and confirmation of the data license.

Data preparation. The diversity of object categories is important for training models for falling object detection around building. As we have stated above, the falling objects in our dataset cover a number of common classes, including clothes, shoes, kitchen waste, books, spitballs, bottles, packaging bags, and packaging boxes. Each object category also includes a rich variety of object instances. For example, the category of kitchen waste includes banana peels, uneaten apples, etc. Besides, light intensity varies with weather condition changes, which would affect the detection performance of falling objects. In addition, the appearance difference between the falling object and the background in a cloudy scene is smaller than that in a fair scene, and raindrops in rainy scenes will also affect the detection accuracy.

Data Collection. We recruit seven volunteers and spend a year and a half to collect the video data. We throw objects from the high-rise buildings of the corresponding university, and use a wide dynamic range camera, equipped with a $1/3''$ progressive scanning CMOS sensor and dot matrix LED infrared lamp to record the whole process of these events. The highest output video quality of the camera is $2592 \times 1520 @ 30 \text{ FPS}$. The motion blur caused by the high-speed moving objects can be reduced if using a global-shutter and high-FPS CMOS. However, this expensive CMOS produces the KTC noise [76]. Besides, it generates more video frames per second, leading to a higher storage cost. More importantly, the already installed cameras around the world for monitoring the falling object are mostly equipped with the general economic sensors. We therefore do not use the camera with global-shutter and high-FPS CMOS to capture video data.

Data format. The annotation format of our dataset is PASCAL VOC [77] style, which is one of the most popular dataset annotation formats. The detailed data format is provided at <https://fadedataset.github.io/FADE.github.io/document.html>.

Data Annotation. The annotation process lasts for half a year, including two rounds. In the first round, the novice annotator labels the video. In the second round, the expert annotator checks the annotation to improve the quality. Different from the pixel-by-pixel annotation method of the MOD datasets [24], [26], [37], we adopt the annotation manner used in the object detection task to generate the bounding box around each falling object.

C. Dataset division and statistics

Dataset Division. When splitting the dataset, we consider five labels, *i.e.* video resolution, scene, lighting condition, weather condition, and object category, for each video. Videos in the training set, validation set, and testing set include all of these labels. To better test the generalization performance of the algorithm, the scenes in our training set, validation set, and testing set (except for the scenes captured in rainy days) are non-overlapped.

Dataset Statistics. We provide some statistical information about the constructed dataset. First, as shown in Figure 5, to make our FADE dataset with abundant falling object categories, we collect the videos covering various falling objects. The percentage of falling objects with different weights is

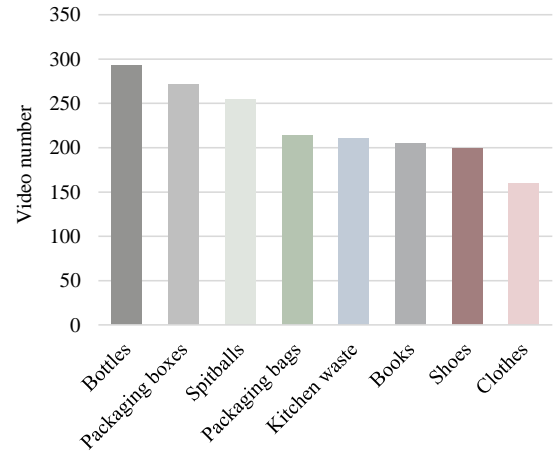


Fig. 5. Statistics of each object category’s video number in our FADE dataset, sorted by descending order.

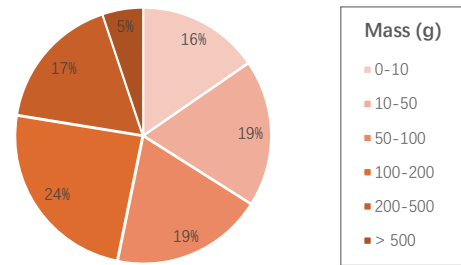


Fig. 6. Percentage of falling objects with different mass in our FADE dataset.

shown in Figure 6. Second, as shown in Table II, most falling objects in our FADE dataset are of small size, where the median area of the falling object is about 20 pixels with the video frame size rescaled to 640×480 .

D. Dataset ethics, license, and maintenance plan.

Ethics. We have full ownership of these videos supplied in our FADE dataset, and all of the collected videos have been authorized for free use by the corresponding university. We inform the seven volunteers, who help us drop the objects from buildings, in advance that their personal information (e.g. faces and hands) may appear in the video, and we get their permission. We conduct two improvements to solve the ethical concerns in our dataset. On the one hand, we have checked all the videos and find that there are 32 videos in our dataset have some people appear. The volunteers who help us to collect the videos are captured in 21 of the videos. For the 21 videos, the volunteers are informed of their appearance and have signed on an informed consent form to allow us to use the videos. The link of this signed informed consent form is: <https://fadedataset.github.io/FADE.github.io/ethic.html>. For the other 11 videos, we remove them from our FADE dataset. On the other hand, we have talked with the corresponding university where we captured the video data and get the authorization. All the videos in our updated FADE dataset can be freely used for the research of falling object detection. We upload the corresponding authorization files to our dataset

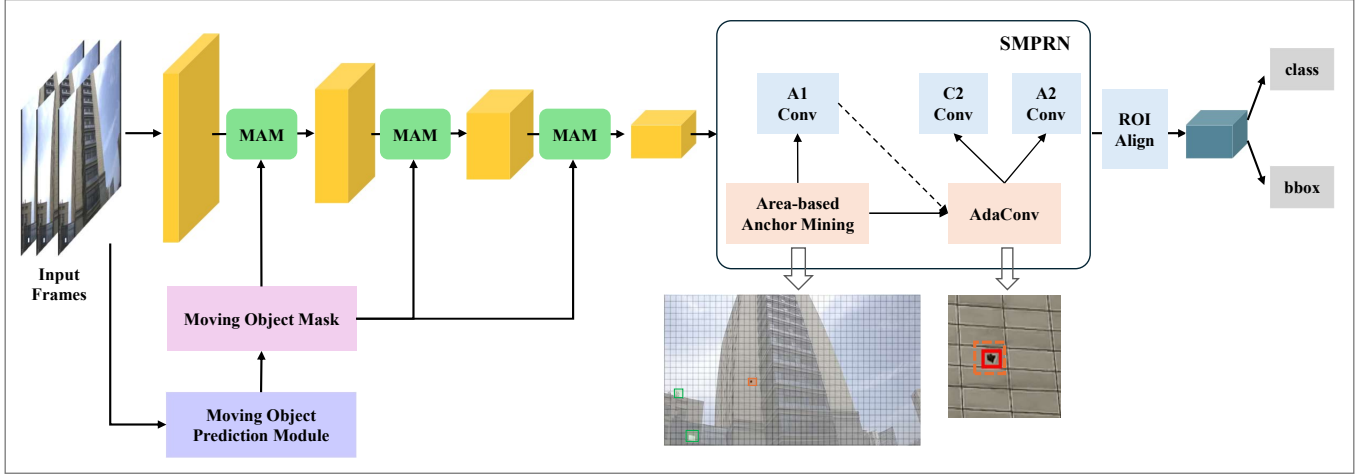


Fig. 7. Overview of our proposed method. Where our method is built upon the Faster R-CNN [78]+FPN [79] framework. “C” and “A” denote classifier and anchor regressor, respectively. “Conv” and “AdaConv” indicate conventional convolution and the adaptive convolution [80] layers, respectively.

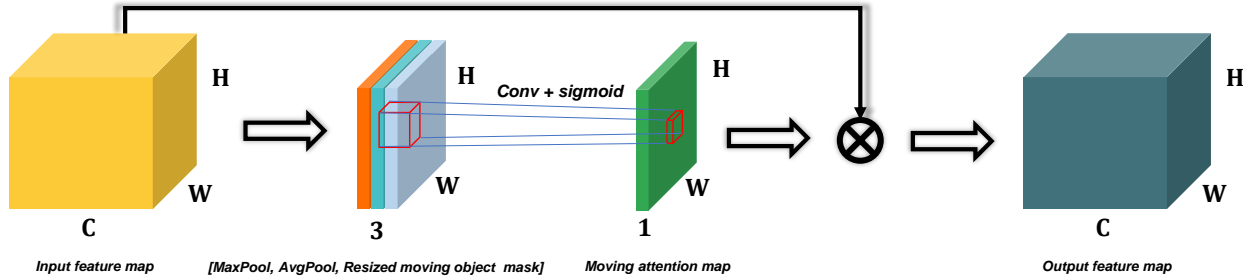


Fig. 8. Details of the moving attention module.

TABLE II
AREA RANGES AND PROPORTIONS OF THE FALLING OBJECTS IN OUR FADE DATASET, SORTED BY ASCENDING ORDER OF THE AREA RANGES. THE VIDEO FRAME SIZE IS RESCALED TO 640×480 .

Range of $area \uparrow$	Number	Proportion %
$0^2 < area \leq 5^2$	37,400	55.34
$5^2 < area \leq 10^2$	18,882	27.94
$10^2 < area \leq 15^2$	7,036	10.41
$15^2 < area \leq 20^2$	2,808	4.15
$area > 20^2$	1,459	2.16

website. The link is: <https://fadedataset.github.io/FADE.github.io/ethic.html>. The authorization files of the corresponding university and the volunteers are available at our dataset website <https://fadedataset.github.io/FADE.github.io/ethic.html>.

License. Our FADE dataset is published under the CC BY-NC-SA 4.0 license, which means everyone can use our dataset for the non-commercial research purpose. Our code is released under the Apache 2.0 license.

Data maintenance and long-term preservation. Our dataset can be downloaded at the website <https://fadedataset.github.io/FADE.github.io/download.html>. We will upload all the video data of our dataset if the paper could be accepted. Our dataset will be maintained for a long time. The corresponding author will provide the support and can be contacted via e-mail. We plan to add more data to perfect our dataset in future.

E. Evaluation metrics

We utilize the precision, recall, and F-measure to compare the performance of different methods, including the tasks of MOD, generic object detection, and video object detection. Since the object size in our dataset FADE is small, we treat a detection as a true positive if its IoU with the GT is larger than 0.3. The F-measure is defined as:

$$F\text{-measure} = \frac{(1 + \beta^2) \cdot \text{precision} \cdot \text{recall}}{\beta^2 \cdot \text{precision} + \text{recall}}. \quad (1)$$

In addition, we set the positive real factor $\beta = 1$, when we calculate the F-measure.

Locating the falling incident temporally is crucial to find out the perpetrator who throws the falling object. We therefore design a useful metric named time range overlap (TRO) to evaluate the ability of the algorithm in this regard. The design of TRO is inspired by the DER (Diarization Error Rate) [81] in the speaker diarization task. The TRO is defined as:

$$TRO = \frac{TR_p \cap TR_{gt}}{TR_p \cup TR_{gt}}, \quad (2)$$

$$TR_p = [T_p^B, T_p^E], TR_{gt} = [T_{gt}^B, T_{gt}^E], \quad (3)$$

where TR_p indicates the predicted time range and TR_{gt} denotes the GT time range. T_p^B and T_{gt}^B are the predicted and the GT beginning time of a falling incident, respectively. T_p^E

and T_{gt}^E separately indicates the predicted and the GT ending time of a falling incident.

IV. PROPOSED METHOD

A. Overview

Generic object detection methods are capable of effectively utilizing appearance features to detect objects. However, for the FODB task, the falling objects are usually small and moving at high speed, making it hard to detect them solely based on the appearance features. To address this issue, we propose a method named FADE-Net, which utilizes motion cues to complement appearance features, as well as generate high-quality proposals for small objects. Specifically, we integrate Moving Attention Modules (MAM) with Small-Object Mining RPN (SMRPN) into a generic object detection method, *i.e.* Faster R-CNN [78]+FPN [79], as shown in Figure 7.

B. Moving attention module (MAM)

To begin with, we employ the moving object prediction module which utilizes the MOD method MOG2 [42] to generate moving object masks for consecutive video frames. MOG2 uses a Gaussian mixture model to imitate background for localizing moving objects. A moving object mask provides candidate moving object regions in a frame. The moving object mask is input to several attention modules for generating attention masks. To recall all the possible moving objects, we choose a relative low threshold for MOG2 to produce the moving object masks.

Then, we introduce three attention modules into the backbone as shown in Figure 7. Each attention module takes the feature map from its preceding layer and the moving object mask from the moving object prediction module as input and outputs an attention map which is multiplied with the feature map to highlight the moving object regions in the feature map. The detailed structure of an attention module is shown in Figure 8. Let F be the feature map of size $H \times W \times C$ from the preceding layer of an attention layer. The moving object mask is resized to the size of $H \times W \times 1$, and we denote the resized moving object mask by M . We apply max pooling and average pooling to F , respectively. The outputs are concatenated with the resized moving object mask and fed to a convolution layer followed by Sigmoid activation to generate a moving attention map. The generation process of the moving attention map (MAP) can be expressed as:

$$MAP = \sigma \left(f^{Conv} ([AvgPool(F), MaxPool(F), M]) \right). \quad (4)$$

The kernel size of the convolution layer is set to 7×7 , and σ represents the Sigmoid function.

C. Small-Object Mining RPN (SMRPN)

We introduce Small-Object Mining RPN (SMRPN), a region proposal network designed to tackle the limitations of existing RPN approaches [78], [82] in handling small objects. Inspired by Cascade RPN [80], SMRPN performs a multi-stage regression process to refine the proposals iteratively. To

address the issue of insufficient and low-quality proposals for small objects, SMRPN employs an area-based anchor mining strategy with a dynamic threshold at the first stage [83]. The threshold can be computed as:

$$Threshold = \max \left(0.20, 0.15 + \alpha \cdot \log \frac{\sqrt{w \cdot h}}{5} \right) \quad (5)$$

where α denotes a scale factor and is set to a default value of 0.2 in our task. The term 5 refers to the minimal area definition of our FADE dataset, ensuring sufficient positive samples for objects of various sizes. The max operation keeps the optimization from being overwhelmed via low quality priors. Moreover, by using the proposed continuous threshold, the model can determine positive samples more smoothly.

Additionally, unlike Cascade RPN, which relies on a single feature pyramid level, SMRPN leverages features from all levels to perform the initial regression, and the information for objects at different scales can be effectively captured accordingly. Following, based on the captured offsets, an adaptive convolution [80] is used to align the anchor and target feature to obtain more refined regression, ultimately generating high-quality proposals for small objects. Consequently, this method is valid for handling the challenges posed by small object detection, paving the way for improving the accuracy of FODB in FADE.

V. EXPERIMENTS

A. Ablation study on the proposed method

In this part, we conduct ablation studies to evaluate the effectiveness of each module in our proposed method FADE-Net. As shown in Table III, both accuracy and recall are improved when adopting SMRPN. Notably, the recall is boosted by more than 20% (26.34% vs 46.53%). This indicates that multi-stage cascade refinement enhances the detection accuracy. Additionally, employing a dynamic area-based anchor mining strategy in the initial stage helps avoiding missed detection of small objects. The adoption of MAM resulted in a significant increase of 38.06% in the recall rate. This indicates that incorporating moving object regions as an attention mask in the detection network effectively captures high-speed falling objects. The simultaneous usage of SMRPN and MAM further enhances the detection performance, suggesting that these two modules are complementary. This improvement shows that the ability to detect small objects and capture trajectories of moving objects contributes to the effectiveness of falling object detection around buildings.

B. Performance in the testing set

To provide a comprehensive benchmark, we conduct extensive experiments on FADE. Various state-of-the-art methods are evaluated, including our method FADE-Net, 5 generic object detection methods, 9 MOD methods and 2 video object detection methods. We use the metrics defined in section III-E for performance evaluation. We specify the implementation details of all algorithms (requirements, hyperparameters, and training details) at <https://github.com/Zhengbo-Zhang/FADE>.

TABLE III

PERFORMANCE OF DIFFERENT MODULES IN THE PROPOSED FADE-NET ON THE TESTING SET OF OUR FADE DATASET. THE BEST PERFORMANCES ARE HIGHLIGHTED IN BOLD.

Faster R-CNN+FPN	SMRPN	MAM	F-measure	Precision	Recall	TRO
✓			35.52	54.50	26.34	32.44
✓	✓		53.41	62.67	46.53	39.12
✓		✓	61.67	59.16	64.40	47.21
✓	✓	✓	72.03	73.48	70.65	51.75

TABLE IV

PERFORMANCE OF DIFFERENT METHODS ON THE TESTING SET OF OUR FADE DATASET. THE BEST AND SECOND BEST PERFORMANCES ARE HIGHLIGHTED IN BOLD AND UNDERLINE, RESPECTIVELY. DLA34 (DCNv2 [84]) [85] INDICATES THAT SOME OF THE CONVOLUTIONS IN THE DLA34 NETWORK ARE REPLACED BY DEFORMABLE CONVOLUTION v2 (DCNv2). FGFA (FlowNet [86]) [87], FGFA (PWC-NET [88]) [87], AND FGFA (RAFT [89]) [87] RESPECTIVELY INDICATE FGFA BASED ON THE OPTICAL FLOW METHODS OF FLOWNET, PWC-NET, AND RAFT.

Method	Type	F-measure	Precision	Recall	TRO
FADE-Net (Ours)	MOD-based Generic Object Detection	72.03	73.48	70.65	51.75
Faster R-CNN [78]+FPN [79]	Generic Object Detection	35.52	54.50	26.34	32.44
YOLOv5 [90]	Generic Object Detection	33.64	54.75	24.28	34.09
DLA34 (DCNv2 [84]) [85]	Generic Object Detection	22.57	20.05	25.80	24.66
DETR [91]	Generic Object Detection	29.95	49.45	21.48	26.87
swin-B [92]	Generic Object Detection	<u>36.93</u>	<u>57.32</u>	27.25	36.58
MOG [93]	Moving Object Detection	17.93	12.82	29.82	20.95
MOG2 [42]	Moving Object Detection	24.48	18.96	34.53	47.98
GMG [94]	Moving Object Detection	2.07	1.14	10.82	14.60
Vibe [8]	Moving Object Detection	15.20	14.61	15.85	23.76
CNT [95]	Moving Object Detection	12.88	19.17	9.70	17.21
FMOD [96]	Moving Object Detection	0.76	6.69	1.36	16.02
KNN [97]	Moving Object Detection	0.72	0.36	30.52	34.16
GSOC [98]	Moving Object Detection	0.61	0.32	10.15	16.18
LSBP [99]	Moving Object Detection	0.12	0.06	6.69	12.36
MEGA [100]	Video Object Detection	5.08	2.64	<u>65.57</u>	<u>48.18</u>
FGFA (FlowNet [86]) [87]	Video Object Detection	0.23	0.12	33.97	46.70
FGFA (PWC-Net [88]) [87]	Video Object Detection	0.20	0.10	32.01	45.54
FGFA (RAFT [89]) [87]	Video Object Detection	0.14	0.07	30.09	43.03

Our proposed FADE-Net achieves the highest performance across all four metrics (see Table IV). During the training process, the CNN generates feature maps that are significantly smaller than the original image, making it is challenging for generic object detection methods to capture features of small objects. However, the statistical data presented in Table II reveals that the falling objects in our dataset are of small size. Our FADE-Net benefits from multi-stage proposal refinement and area-based anchor mining strategy, enabling better detection of small objects. Furthermore, motion blur caused by the fast motion of falling objects can reduce the recall of image-based detection models. Our FADE-Net focuses on determining the candidate motion object regions in adjacent frames and incorporates motion-attention masks at various stages of the network, providing more accurate detection.

Despite being the best MOD method, MOG2 [42] still exhibits a significant precision gap compared to our proposed FADE-Net. The reason for this is that our FADE-Net learns rich appearance features of falling objects during offline training and effectively extracts these features during the inference process, which greatly aids in falling object detection. In contrast, the MOD method can only update the model online during the inference process and is unable to leverage this valuable prior knowledge. This causes MOG2 to detect some moving objects that are not falling objects, such as clouds

and shadows. The detection results of LSBP [99] contain a large number of ghost regions (trailing regions at the tail of the fast moving object which are outside the contour of the fast moving object) [101], leading to its worst precision and F-measure.

MEGA [100] combines the global semantic information with the local localization information, as well as utilizes more key frames in the video for detection. It therefore is very sensitive to detect the falling object and to locate the beginning-ending time of the FODB incident. It achieves the second best recall and TRO performance. Since MEGA is not aimed at small object detection, its network cannot learn the appearance features of the small falling objects well. In addition, since the falling objects move too fast and the motion occupies several video frames, the motion region is easily submerged in the time series. As a result, MEGA gets low precision in the constructed FADE dataset.

C. Analysis of optical flow based methods in FODB

Optical flow is good at estimating motion information in video by capturing the pixel-level dense motion field. It is widely used in many video tasks, e.g. action recognition [104]–[107] and MOD [100], and makes good performance. However, as shown in Table IV, the optical flow based methods FGFA (FlowNet [86]) [87] (the original method using FlowNet

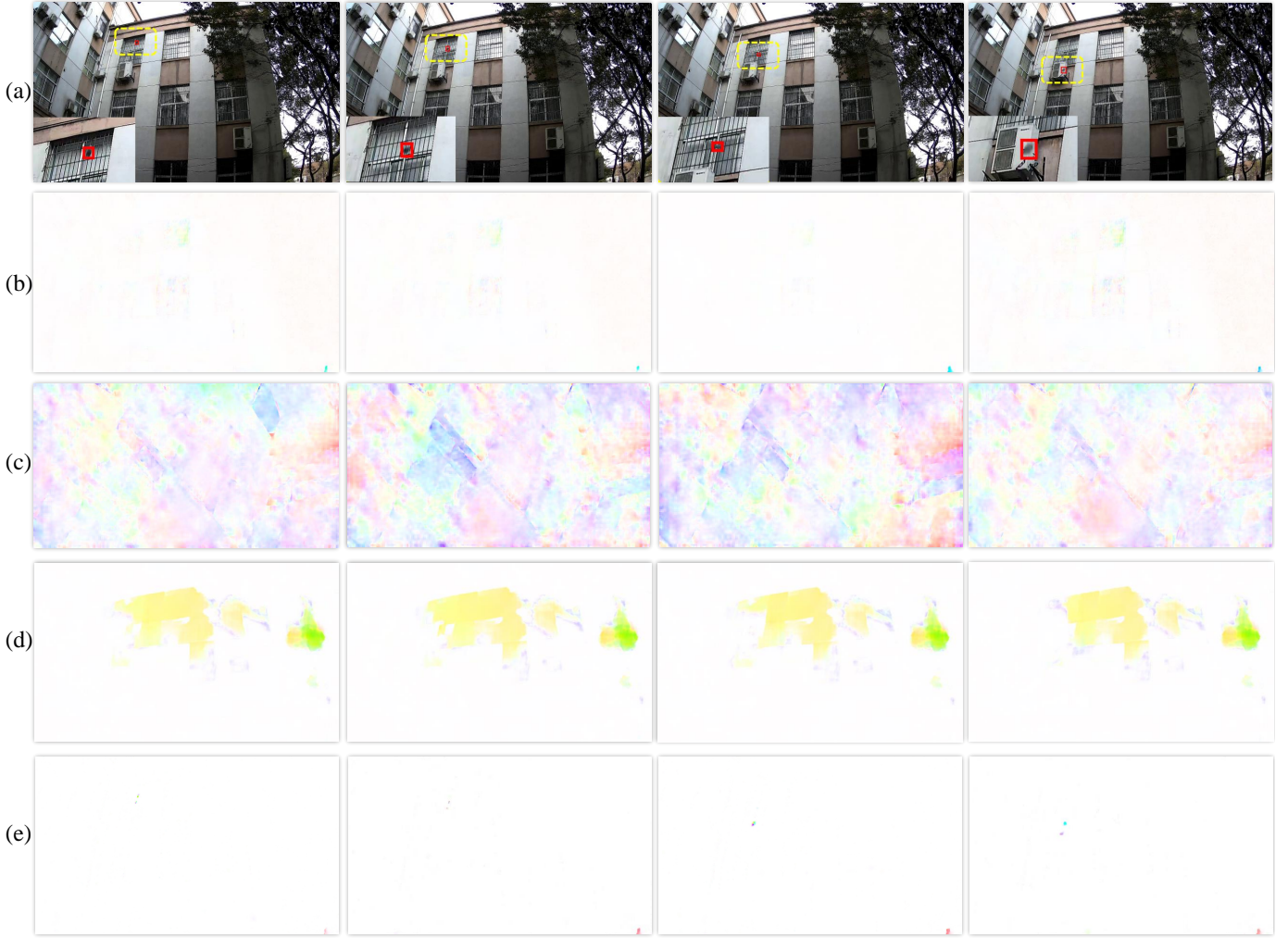


Fig. 9. Video frames in our FADE dataset and their corresponding optical flow field images estimated by different optical flow methods. (a) Four consecutive video frames with a falling object from the building in our dataset. (b), (c), (d), and (e) The corresponding optical flow images computed by FlowNet 2.0 [102], RAFT [89], PWC-Net [88], and TV-L1 [103]. To see the moving object in the falling object detection task clearly, we enlarge the object in the frame and place it in the lower left corner of the video frame.

to compute optical flow), FGFA (PWC-Net [88]) [87], and FGFA (RAFT [89]) [87], do not obtain the expected performance in falling object detection in our FADE (the F-measure of FGFA (RAFT) is the second worst). To find out the reason, we apply a variety of representative optical flow methods, e.g. FlowNet, PWC-Net, and RAFT to generate the optical flow images in FADE for comparison, and we provide these images in Figure 9. By observing these optical flow images estimated by the deep learning based optical flow algorithms [86], [88], [89], we find that some optical flow images are chaotic, resulting in the background and the falling object being difficult to be distinguished. Besides, the displacement of falling object is inaccurately computed.

We think that there are two main reasons for the poor performance of the optical flow based method in FODB task. The first reason is motion blur and occlusion. Appearance of a falling object constantly changes due to the motion blur caused by the fast movement as well as the occlusion caused by trees, neighboring buildings, et al. in the falling process.

The second is large displacements. The falling object produces large displacements due to fast movement. With the challenges of motion blur, occlusion, and large displacements, the optical flow is hard to be estimated precisely.

D. Visualization Results

Optical flow images. As can be seen in Figure 9, we plot the optical flow images generated by 4 popular optical flow methods (FlowNet 2.0 [102], RAFT [89], PWC-Net [88], and TV-L1 [103]) to visualize the performance of the optical flow in our FADE dataset. The first three groups of optical flow images, estimated by the deep learning based optical flow algorithms [86], [88], [89], are very confusing, resulting in the background and the moving object being difficult to be distinguished. For the last group (*i.e.* last column) of optical flow images, which are captured by the traditional variational optical flow method [103], the movement of the static background is well estimated, but the motion of the moving objects is also poorly computed.

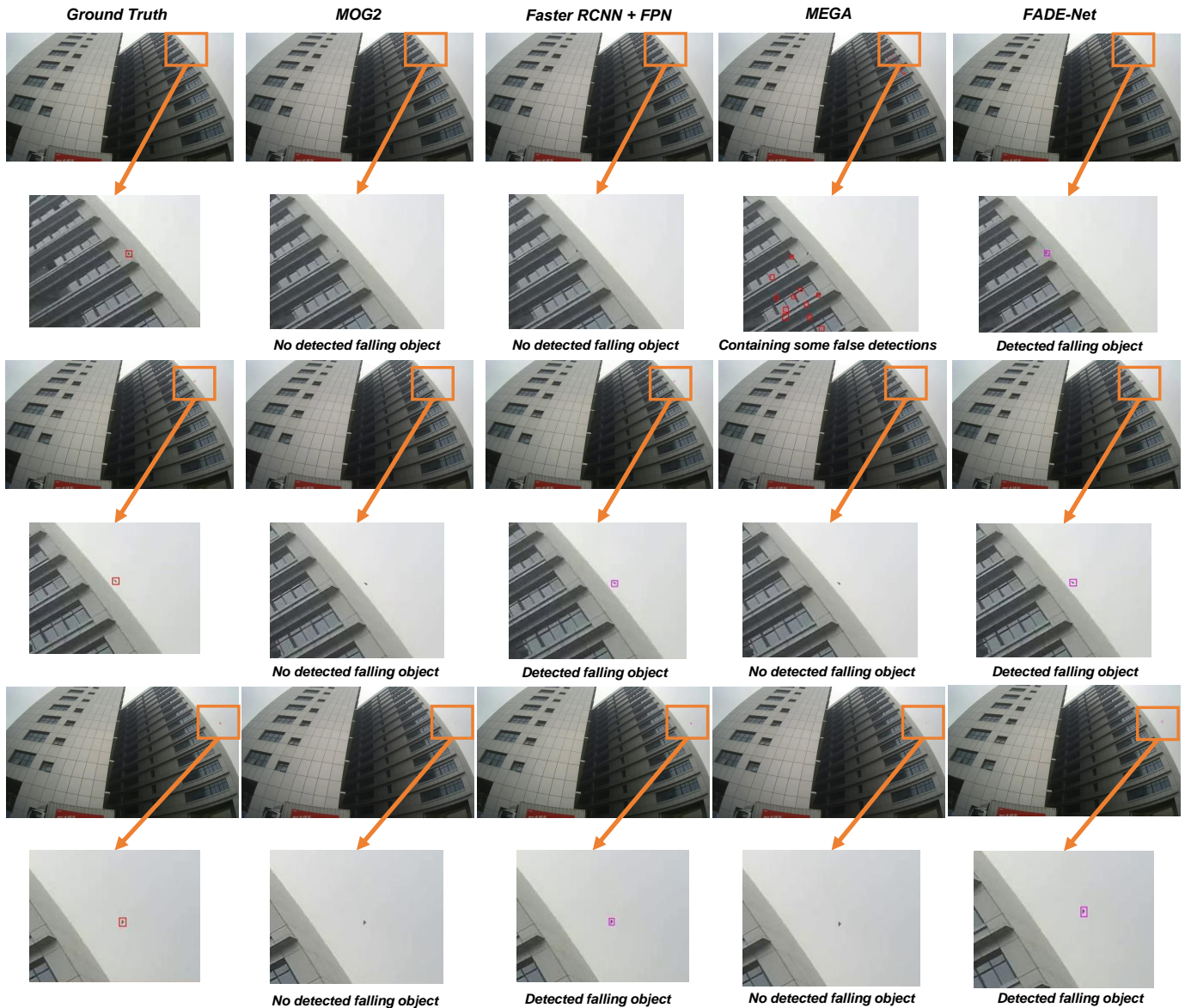


Fig. 10. We show ground-truth and the detection results of MOG2 [42], Faster R-CNN [78] + FPN [79], MEGA [100] and our proposed FADE-Net on three frames sampled from a video. MOG2, Faster R-CNN + FPN and MEGA are representative algorithms of moving object detection, image object detection, and video object detection respectively. In order to illustrate the difference between the detection results more clearly, we enlarge the regions around the falling objects in the frames.

Visualization results of representative methods. Visualization results of the representative moving object detection method (MOG2 [42]), image object detection method (Faster R-CNN [78]+FPN [79]), video object detection method (MEGA [100]), and our proposed FADE-Net are shown in Figure 10. We can find that many detection results of MOG2 only include part of the falling object, because MOG2 can only update the model online in the inference process and cannot make use of the rich appearance features of the falling object in the offline training process. Besides, the post-processing of MOG2 includes the opening operation in morphology, which would eliminate the small detection. Thus, some small falling objects on the video frame cannot be detected. The accuracy of

Faster R-CNN + FPN is higher than the other two algorithms, and it is also difficult to detect some small falling objects. In addition, the motion blur caused by the fast motion also increases the detection difficulty of the image-based detection model. The accuracy of MEGA is the worst. This method does not learn the appearance features and motion information of the falling object well during the training process, and the lack of non-maximum suppression processing further reduces its accuracy. Our proposed method FADE-Net achieves the best performance in all three video sequences, benefiting from seamlessly integrating generic object detection and motion information in videos. The moving attention module designed by us allows the network to assign adaptive weights to different

regions according to the motion information of the image, effectively reducing false detections in the image.

VI. LIMITATION

Generally, our dataset has two main limitations:

The diversity of scenes. Although our dataset includes a large amount of video data and diverse categories, the scenarios can still be further enriched. Consequently, gathering video data in more scenarios to enrich our dataset is a successive future work for FODB.

The baseline method. Our baseline method considers object motion within a short temporal range (less than 1 second). Consequently, exploring to leverage long-term temporal motion information to further boost the detection accuracy is another successive future work for FODB.

VII. CONCLUSION

In this work, we propose a new large-scale video dataset termed FADE for falling object detection around buildings (FODB). It contains 1,881 videos and 164,314 video frames. The videos in FADE include various categories of objects and are captured under diverse scenes, weather conditions, lighting conditions, and video resolutions. Notably, different from the existing MOD datasets, our FADE is the first dataset specialized for FODB. Additionally, we introduce a new baseline method called FADE-Net, which seamlessly integrates motion information capturing and small-sized proposal mining into the detection network. Furthermore, to evaluate the FODB algorithms more effectively, we design an evaluation metric called TRO, which measures the algorithm's ability to locate the beginning and ending times of falling incidents.

We provide a comprehensive benchmark that includes our FADE-Net baseline method, popular MOD methods, generic object detection methods, and video object detection methods. Extensive experimental results demonstrate that FODB is a challenging task in the presence of complex backgrounds and motion blur, and validating the effectiveness of our explored baseline method FADE-Net. The FADE dataset, with its diverse videos, will promote the progress of FODB and may also be useful for the investigation of MOD, generic object detection, and video object detection. In future, we will continue to refine and expand the dataset FADE, and explore more advanced FODB methods.

ACKNOWLEDGMENTS

This work was supported by the Natural Science Fund for Distinguished Young Scholars of Hubei Province under Grant 2022CFA075, the National Natural Science Foundation of China (NSFC) under Grant 62106177, and the Fundamental Research Funds for the Central Universities under Grant 2042023KF0180. The numerical calculation was supported by the super-computing system in the Super-computing Center of Wuhan University.

REFERENCES

- [1] U. B. of Labor Statistics, "Commonly used statistics," Website, 2019, <https://www.osha.gov/data/commonstats>.
- [2] D. Morin, *Introduction to Classical Mechanics*. Cambridge University Press, 2008.
- [3] C. of Virginia, "Code of virginia," Website, 1990, <https://law.lis.virginia.gov/vacode/title18.2/chapter4/section18.2-51.3/>.
- [4] A. H. T. Council, "Laws," Website, 2023, <https://www.ahtc.sg/by-laws/>.
- [5] C. Daily, "Legal document issued by the supreme people's court," Website, 2019, <https://www.chinadaily.com.cn/a/201911/14/WS5dccc956a310cf3e3557757b.html>.
- [6] N. Babaguchi, A. Cavallaro, R. Chellappa, F. Dufaux, and L. Wang, "Guest editorial: special issue on intelligent video surveillance for public security and personal privacy," *IEEE Transactions on Information Forensics and Security*, vol. 8, no. 10, pp. 1559–1561, 2013.
- [7] S. Aslani and H. Mahdavi-Nasab, "Optical flow based moving object detection and tracking for traffic surveillance," *International Journal of Electrical, Computer, Energetic, Electronic and Communication Engineering*, vol. 7, no. 9, pp. 1252–1256, 2013.
- [8] O. Barnich and M. Van Droogenbroeck, "Vibe: A universal background subtraction algorithm for video sequences," *IEEE Transactions on Image processing*, vol. 20, no. 6, pp. 1709–1724, 2010.
- [9] C. Stauffer and W. E. L. Grimson, "Adaptive background mixture models for real-time tracking," in *Proceedings. 1999 IEEE computer society conference on computer vision and pattern recognition (Cat. No. PR00149)*, vol. 2. IEEE, 1999, pp. 246–252.
- [10] W. Sultani, C. Chen, and M. Shah, "Real-world anomaly detection in surveillance videos," in *Proceedings of the IEEE conference on computer vision and pattern recognition*, 2018, pp. 6479–6488.
- [11] J. T. Zhou, J. Du, H. Zhu, X. Peng, Y. Liu, and R. S. M. Goh, "AnomalyNet: An anomaly detection network for video surveillance," *IEEE Transactions on Information Forensics and Security*, vol. 14, no. 10, pp. 2537–2550, 2019.
- [12] G. Chen, P. Liu, Z. Liu, H. Tang, L. Hong, J. Dong, J. Conradt, and A. Knoll, "Neuroaed: Towards efficient abnormal event detection in visual surveillance with neuromorphic vision sensor," *IEEE Transactions on Information Forensics and Security*, vol. 16, pp. 923–936, 2020.
- [13] G. Yu, S. Wang, Z. Cai, X. Liu, E. Zhu, and J. Yin, "Video anomaly detection via visual cloze tests," *IEEE Transactions on Information Forensics and Security*, 2023.
- [14] Z. Zheng, L. Zheng, and Y. Yang, "Pedestrian alignment network for large-scale person re-identification," *IEEE Transactions on Circuits and Systems for Video Technology*, vol. 29, no. 10, pp. 3037–3045, 2018.
- [15] K. Navaneet, R. K. Sarvadevabhatla, S. Shekhar, R. V. Babu, and A. Chakraborty, "Operator-in-the-loop deep sequential multi-camera feature fusion for person re-identification," *IEEE Transactions on Information Forensics and Security*, vol. 15, pp. 2375–2385, 2019.
- [16] Y. Du, C. Lei, Z. Zhao, Y. Dong, and F. Su, "Video-based visible-infrared person re-identification with auxiliary samples," *IEEE Transactions on Information Forensics and Security*, vol. 19, pp. 1313–1325, 2023.
- [17] A. Brunetti, D. Buongiorno, G. F. Trotta, and V. Bevilacqua, "Computer vision and deep learning techniques for pedestrian detection and tracking: A survey," *Neurocomputing*, vol. 300, pp. 17–33, 2018.
- [18] Z. Sun, J. Chen, L. Chao, W. Ruan, and M. Mukherjee, "A survey of multiple pedestrian tracking based on tracking-by-detection framework," *IEEE Transactions on Circuits and Systems for Video Technology*, vol. 31, no. 5, pp. 1819–1833, 2020.
- [19] S. A. Kumar, E. Yaghoubi, A. Das, B. Harish, and H. Proença, "The p-destre: A fully annotated dataset for pedestrian detection, tracking, and short/long-term re-identification from aerial devices," *IEEE Transactions on Information Forensics and Security*, vol. 16, pp. 1696–1708, 2020.
- [20] B. Degardin, V. Lopes, and H. Proença, "Regina—reasoning graph convolutional networks in human action recognition," *IEEE Transactions on Information Forensics and Security*, vol. 16, pp. 5442–5451, 2021.
- [21] Z. Tu, J. Zhang, H. Li, Y. Chen, and J. Yuan, "Joint-bone fusion graph convolutional network for semi-supervised skeleton action recognition," *IEEE Transactions on Multimedia*, 2022.
- [22] Z. Tu, Z. Huang, Y. Chen, D. Kang, L. Bao, B. Yang, and J. Yuan, "Consistent 3d hand reconstruction in video via self-supervised learning," *IEEE Transactions on Pattern Analysis and Machine Intelligence*, vol. 45, no. 8, pp. 9469–9485, 2023.
- [23] J. Zhang, Z. Tu, J. Weng, J. Yuan, and B. Du, "A modular neural motion retargeting system decoupling skeleton and shape perception," *IEEE Transactions on Pattern Analysis and Machine Intelligence*, 2024.

- [24] S. Brutzer, B. Höferlin, and G. Heidemann, "Evaluation of background subtraction techniques for video surveillance," in *CVPR 2011*. IEEE, 2011, pp. 1937–1944.
- [25] Y. Wang, P.-M. Jodoin, F. Porikli, J. Konrad, Y. Benezeth, and P. Ishwar, "Cdnnet 2014: An expanded change detection benchmark dataset," in *Proceedings of the IEEE conference on computer vision and pattern recognition workshops*, 2014, pp. 387–394.
- [26] C. Li, X. Wang, L. Zhang, J. Tang, H. Wu, and L. Lin, "Weighted low-rank decomposition for robust grayscale-thermal foreground detection," *IEEE Transactions on Circuits and Systems for Video Technology*, vol. 27, no. 4, pp. 725–738, 2016.
- [27] C. Cuevas, E. M. Yáñez, and N. García, "Labeled dataset for integral evaluation of moving object detection algorithms: Lasiesta," *Computer Vision and Image Understanding*, vol. 152, pp. 103–117, 2016.
- [28] T.-Y. Lin, M. Maire, S. Belongie, J. Hays, P. Perona, D. Ramanan, P. Dollár, and C. L. Zitnick, "Microsoft coco: Common objects in context," in *Computer Vision—ECCV 2014: 13th European Conference, Zurich, Switzerland, September 6–12, 2014, Proceedings, Part V 13*. Springer, 2014, pp. 740–755.
- [29] K. Toyama, J. Krumm, B. Brumitt, and B. Meyers, "Wallflower: Principles and practice of background maintenance," in *Computer Vision, 1999. The Proceedings of the Seventh IEEE International Conference on*, 1999.
- [30] D. Tsai, M. Flagg, A. Nakazawa, and J. M. Rehg, "Motion coherent tracking using multi-label mrf optimization," *International journal of computer vision*, vol. 100, no. 2, pp. 190–202, 2012.
- [31] L. Li, W. Huang, I. Y.-H. Gu, and Q. Tian, "Statistical modeling of complex backgrounds for foreground object detection," *IEEE Transactions on Image Processing*, vol. 13, no. 11, pp. 1459–1472, 2004.
- [32] P. Ochs, J. Malik, and T. Brox, "Segmentation of moving objects by long term video analysis," *IEEE transactions on pattern analysis and machine intelligence*, vol. 36, no. 6, pp. 1187–1200, 2013.
- [33] F. Li, T. Kim, A. Humayun, D. Tsai, and J. M. Rehg, "Video segmentation by tracking many figure-ground segments," in *Proceedings of the IEEE international conference on computer vision*, 2013, pp. 2192–2199.
- [34] N. Goyette, P.-M. Jodoin, F. Porikli, J. Konrad, and P. Ishwar, "Changetection.net: A new change detection benchmark dataset," in *2012 IEEE computer society conference on computer vision and pattern recognition workshops*. IEEE, 2012, pp. 1–8.
- [35] A. Vacavant, T. Chateau, A. Wilhelm, and L. Lequievre, "A benchmark dataset for outdoor foreground/background extraction," in *Asian Conference on Computer Vision*. Springer, 2012, pp. 291–300.
- [36] F. Perazzi, J. Pont-Tuset, B. McWilliams, L. Van Gool, M. Gross, and A. Sorkine-Hornung, "A benchmark dataset and evaluation methodology for video object segmentation," in *Proceedings of the IEEE conference on computer vision and pattern recognition*, 2016, pp. 724–732.
- [37] L. Maddalena and A. Petrosino, "Towards benchmarking scene background initialization," in *International conference on image analysis and processing*. Springer, 2015, pp. 469–476.
- [38] R. Cucchiara, C. Grana, G. Neri, M. Piccardi, and A. Prati, "The sakbot system for moving object detection and tracking," in *Video-based surveillance systems*. Springer, 2002, pp. 145–157.
- [39] K. A. Joshi and D. G. Thakore, "A survey on moving object detection and tracking in video surveillance system," *International Journal of Soft Computing and Engineering*, vol. 2, no. 3, pp. 44–48, 2012.
- [40] C. Poppe, S. De Bruyne, T. Paridaens, P. Lambert, and R. Van de Walle, "Moving object detection in the h. 264/avc compressed domain for video surveillance applications," *Journal of Visual Communication and Image Representation*, vol. 20, no. 6, pp. 428–437, 2009.
- [41] S. Varadarajan, P. Miller, and H. Zhou, "Spatial mixture of gaussians for dynamic background modelling," in *2013 10th IEEE international conference on advanced video and signal based surveillance*. IEEE, 2013, pp. 63–68.
- [42] Z. Zivkovic, "Improved adaptive gaussian mixture model for background subtraction," in *Proceedings of the 17th International Conference on Pattern Recognition, 2004. ICPR 2004.*, vol. 2. IEEE, 2004, pp. 28–31.
- [43] F. El Baf, T. Bouwmans, and B. Vachon, "Fuzzy integral for moving object detection," in *2008 IEEE International Conference on Fuzzy Systems (IEEE World Congress on Computational Intelligence)*. IEEE, 2008, pp. 1729–1736.
- [44] H. Tahani and J. M. Keller, "Information fusion in computer vision using the fuzzy integral," *IEEE Transactions on systems, Man, and Cybernetics*, vol. 20, no. 3, pp. 733–741, 1990.
- [45] K. Lin, S.-C. Chen, C.-S. Chen, D.-T. Lin, and Y.-P. Hung, "Abandoned object detection via temporal consistency modeling and back-tracing verification for visual surveillance," *IEEE Transactions on Information Forensics and Security*, vol. 10, no. 7, pp. 1359–1370, 2015.
- [46] Y. Yang, A. Loquercio, D. Scaramuzza, and S. Soatto, "Unsupervised moving object detection via contextual information separation," in *Proceedings of the IEEE/CVF Conference on Computer Vision and Pattern Recognition*, 2019, pp. 879–888.
- [47] K. Thanikasalam, C. Fookes, S. Sridharan, A. Ramanan, and A. Pini-diyaarachchi, "Target-specific siamese attention network for real-time object tracking," *IEEE Transactions on Information Forensics and Security*, vol. 15, pp. 1276–1289, 2019.
- [48] F. Shang, J. Cheng, Y. Liu, Z.-Q. Luo, and Z. Lin, "Bilinear factor matrix norm minimization for robust pca: Algorithms and applications," *IEEE transactions on pattern analysis and machine intelligence*, vol. 40, no. 9, pp. 2066–2080, 2017.
- [49] N. Vaswani, T. Bouwmans, S. Javed, and P. Narayanamurthy, "Robust subspace learning: Robust pca, robust subspace tracking, and robust subspace recovery," *IEEE signal processing magazine*, vol. 35, no. 4, pp. 32–55, 2018.
- [50] Y. Yu, Y. Xiong, W. Huang, and M. R. Scott, "Deformable siamese attention networks for visual object tracking," in *Proceedings of the IEEE/CVF conference on computer vision and pattern recognition*, 2020, pp. 6728–6737.
- [51] Z. Zhang, L. Xu, D. Peng, H. Rahmani, and J. Liu, "Diff-tracker: Text-to-image diffusion models are unsupervised trackers," in *European Conference on Computer Vision*. Springer, 2024.
- [52] M. Danelljan, L. V. Gool, and R. Timofte, "Probabilistic regression for visual tracking," in *Proceedings of the IEEE/CVF conference on computer vision and pattern recognition*, 2020, pp. 7183–7192.
- [53] B. Yan, H. Peng, J. Fu, D. Wang, and H. Lu, "Learning spatio-temporal transformer for visual tracking," in *Proceedings of the IEEE/CVF international conference on computer vision*, 2021, pp. 10448–10457.
- [54] Y. Dong and G. N. DeSouza, "Adaptive learning of multi-subspace for foreground detection under illumination changes," *Computer Vision and Image Understanding*, vol. 115, no. 1, pp. 31–49, 2011.
- [55] A. Krizhevsky, I. Sutskever, and G. E. Hinton, "Imagenet classification with deep convolutional neural networks," *Advances in neural information processing systems*, vol. 25, 2012.
- [56] Z. Zhang, Y. Zhou, J. Gong, J. Liu, and Z. Tu, "Instance temperature knowledge distillation," *arXiv preprint arXiv:2407.00115*, 2024.
- [57] D. Peng, Z. Zhang, P. Hu, Q. Ke, D. Yau, and J. Liu, "Harnessing text-to-image diffusion models for category-agnostic pose estimation," in *European Conference on Computer Vision*. Springer, 2024.
- [58] J. Long, E. Shelhamer, and T. Darrell, "Fully convolutional networks for semantic segmentation," in *Proceedings of the IEEE conference on computer vision and pattern recognition*, 2015, pp. 3431–3440.
- [59] O. Ronneberger, P. Fischer, and T. Brox, "U-net: Convolutional networks for biomedical image segmentation," in *International Conference on Medical image computing and computer-assisted intervention*. Springer, 2015, pp. 234–241.
- [60] M. Braham and M. Van Droogenbroeck, "Deep background subtraction with scene-specific convolutional neural networks," in *2016 international conference on systems, signals and image processing (IWSSIP)*. IEEE, 2016, pp. 1–4.
- [61] J. H. Giraldo, S. Javed, and T. Bouwmans, "Graph moving object segmentation," *IEEE Transactions on Pattern Analysis and Machine Intelligence*, 2020.
- [62] T.-N. Le and A. Sugimoto, "Video salient object detection using spatiotemporal deep features," *IEEE Transactions on Image Processing*, vol. 27, no. 10, pp. 5002–5015, 2018.
- [63] P. W. Patil, K. M. Biradar, A. Dudhane, and S. Murala, "An end-to-end edge aggregation network for moving object segmentation," in *proceedings of the IEEE/CVF conference on computer vision and pattern recognition*, 2020, pp. 8149–8158.
- [64] Z. Zhang, C. Zhou, and Z. Tu, "Distilling inter-class distance for semantic segmentation," *arXiv preprint arXiv:2205.03650*, 2022.
- [65] M. Babae, D. T. Dinh, and G. Rigoll, "A deep convolutional neural network for video sequence background subtraction," *Pattern Recognition*, vol. 76, pp. 635–649, 2018.
- [66] T. Bouwmans, S. Javed, M. Sultana, and S. K. Jung, "Deep neural network concepts for background subtraction: A systematic review and comparative evaluation," *Neural Networks*, vol. 117, pp. 8–66, 2019.
- [67] M. Mandal, V. Dhar, A. Mishra, and S. K. Vipparthi, "3dfir: A swift 3d feature reductionist framework for scene independent change detection," *IEEE Signal Processing Letters*, vol. 26, no. 12, pp. 1882–1886, 2019.

- [68] M. Mandal, V. Dhar, A. Mishra, S. K. Vipparthi, and M. Abdel-Mottaleb, “3dcd: Scene independent end-to-end spatiotemporal feature learning framework for change detection in unseen videos,” *IEEE Transactions on Image Processing*, vol. 30, pp. 546–558, 2020.
- [69] Y. Chen, J. Wang, B. Zhu, M. Tang, and H. Lu, “Pixelwise deep sequence learning for moving object detection,” *IEEE Transactions on Circuits and Systems for Video Technology*, vol. 29, no. 9, pp. 2567–2579, 2017.
- [70] D. Zeng and M. Zhu, “Background subtraction using multiscale fully convolutional network,” *IEEE Access*, vol. 6, pp. 16010–16021, 2018.
- [71] M. Sultana, A. Mahmood, T. Bouwmans, and S. Ki Jung, “Complete moving object detection in the context of robust subspace learning,” in *Proceedings of the IEEE/CVF International Conference on Computer Vision Workshops*, 2019, pp. 0–0.
- [72] M. Sultana, A. Mahmood, S. Javed, and S. K. Jung, “Unsupervised deep context prediction for background estimation and foreground segmentation,” *Machine Vision and Applications*, vol. 30, no. 3, pp. 375–395, 2019.
- [73] B. Zheng, Y. Zhao, C. Y. Joey, K. Ikeuchi, and S.-C. Zhu, “Detecting potential falling objects by inferring human action and natural disturbance,” in *2014 IEEE International Conference on Robotics and Automation (ICRA)*. IEEE, 2014, pp. 3417–3424.
- [74] F. J. Alvarez, J. Urena, M. Mazo, A. Hernández, J. Garcia, and P. Donato, “Ultrasonic sensor system for detecting falling objects on railways,” in *IEEE Intelligent Vehicles Symposium, 2004*. IEEE, 2004, pp. 866–871.
- [75] B. Yang, B. Zhang, Q. Zhang, Z. Wang, M. Dong, and T. Fang, “Automatic detection of falling hazard from surveillance videos based on computer vision and building information modeling,” *Structure and Infrastructure Engineering*, pp. 1–15, 2022.
- [76] S. Lauthermann, A. Lee, J. Stevens, and A. Joshi, “Comparison of global shutter pixels for cmos image sensors,” in *2007 International Image Sensor Workshop*, 2007, p. 8.
- [77] M. Everingham, L. Van Gool, C. K. Williams, J. Winn, and A. Zisserman, “The pascal visual object classes (voc) challenge,” *International journal of computer vision*, vol. 88, no. 2, pp. 303–338, 2010.
- [78] S. Ren et al, “Faster r-cnn: Towards real-time object detection with region proposal networks,” *NeurIPS*, vol. 28, 2015.
- [79] T.-Y. Lin, P. Dollár, R. Girshick, K. He, B. Hariharan, and S. Belongie, “Feature pyramid networks for object detection,” in *CVPR*, 2017, pp. 2117–2125.
- [80] T. Vu, H. Jang, T. X. Pham, and C. Yoo, “Cascade rpn: Delving into high-quality region proposal network with adaptive convolution,” *Advances in neural information processing systems*, vol. 32, 2019.
- [81] F. Yu, S. Zhang, P. Guo, Y. Fu, Z. Du, S. Zheng, W. Huang, L. Xie, Z.-H. Tan, D. Wang et al., “Summary on the icassp 2022 multi-channel multi-party meeting transcription grand challenge,” in *ICASSP 2022-2022 IEEE International Conference on Acoustics, Speech and Signal Processing (ICASSP)*. IEEE, 2022, pp. 9156–9160.
- [82] J. Wang, K. Chen, S. Yang, C. C. Loy, and D. Lin, “Region proposal by guided anchoring,” in *CVPR*, 2019, pp. 2965–2974.
- [83] X. Yuan, G. Cheng, K. Yan, Q. Zeng, and J. Han, “Small object detection via coarse-to-fine proposal generation and imitation learning,” in *ICCV*, 2023, pp. 6317–6327.
- [84] X. Zhu et al, “Deformable convnets v2: More deformable, better results,” in *CVPR*, 2019, pp. 9308–9316.
- [85] F. Yu, D. Wang, E. Shelhamer, and T. Darrell, “Deep layer aggregation,” in *Proceedings of the IEEE conference on computer vision and pattern recognition*, 2018, pp. 2403–2412.
- [86] A. Dosovitskiy, P. Fischer, E. Ilg, P. Hausser, C. Hazirbas, V. Golkov, P. Van Der Smagt, D. Cremers, and T. Brox, “FlowNet: Learning optical flow with convolutional networks,” in *Proceedings of the IEEE international conference on computer vision*, 2015, pp. 2758–2766.
- [87] X. Zhu, Y. Wang, J. Dai, L. Yuan, and Y. Wei, “Flow-guided feature aggregation for video object detection,” in *Proceedings of the IEEE international conference on computer vision*, 2017, pp. 408–417.
- [88] D. Sun, X. Yang, M.-Y. Liu, and J. Kautz, “Pwc-net: Cnns for optical flow using pyramid, warping, and cost volume,” in *Proceedings of the IEEE conference on computer vision and pattern recognition*, 2018, pp. 8934–8943.
- [89] Z. Teed and J. Deng, “Raft: Recurrent all-pairs field transforms for optical flow,” in *European conference on computer vision*. Springer, 2020, pp. 402–419.
- [90] G. Jocher, “Yolov5,” Website, 2020, <https://github.com/ultralytics/yolov5>.
- [91] N. Carion, F. Massa, G. Synnaeve, N. Usunier, A. Kirillov, and S. Zagoruyko, “End-to-end object detection with transformers,” in *European conference on computer vision*. Springer, 2020, pp. 213–229.
- [92] Z. Liu, Y. Lin, Y. Cao, H. Hu, Y. Wei, Z. Zhang, S. Lin, and B. Guo, “Swin transformer: Hierarchical vision transformer using shifted windows,” in *ICCV*, 2021, pp. 10012–10022.
- [93] P. KaewTraKulPong and R. Bowden, “An improved adaptive background mixture model for real-time tracking with shadow detection,” in *Video-based surveillance systems*. Springer, 2002, pp. 135–144.
- [94] A. B. Godbehere, A. Matsukawa, and K. Goldberg, “Visual tracking of human visitors under variable-lighting conditions for a responsive audio art installation,” in *2012 American Control Conference (ACC)*. IEEE, 2012, pp. 4305–4312.
- [95] S. ZEEVI, “Backgroundsubtractorcnt,” Website, 2016, <https://github.com/sagi-z/BackgroundSubtractorCNT>.
- [96] D. Rozumnyi et al, “Fmodetect: Robust detection of fast moving objects,” in *ICCV*, 2021, pp. 3541–3549.
- [97] Z. Zivkovic and F. Van Der Heijden, “Efficient adaptive density estimation per image pixel for the task of background subtraction,” *Pattern recognition letters*, vol. 27, no. 7, pp. 773–780, 2006.
- [98] G. S. of Code, “Backgroundsubtractorgsoc,” Website, 2016, https://docs.opencv.org/4.x/d4/dd5/classcv_1_1bgsegm_1_1BackgroundSubtractorGSOC.html.
- [99] L. Guo, D. Xu, and Z. Qiang, “Background subtraction using local svd binary pattern,” in *Proceedings of the IEEE conference on computer vision and pattern recognition workshops*, 2016, pp. 86–94.
- [100] Y. Chen, Y. Cao, H. Hu, and L. Wang, “Memory enhanced global-local aggregation for video object detection,” in *Proceedings of the IEEE/CVF conference on computer vision and pattern recognition*, 2020, pp. 10337–10346.
- [101] S. H. Shaikh, K. Saeed, and N. Chaki, “Moving object detection using background subtraction,” in *Moving object detection using background subtraction*. Springer, 2014, pp. 15–23.
- [102] E. Ilg, N. Mayer, T. Saikia, M. Keuper, and T. Brox, “FlowNet 2.0: Evolution of optical flow estimation with deep networks,” *2017 IEEE Conference on Computer Vision and Pattern Recognition (CVPR)*, 2017.
- [103] C. Zach, T. Pock, and H. Bischof, “A duality based approach for realtime tv-l1 optical flow,” in *Joint pattern recognition symposium*. Springer, 2007, pp. 214–223.
- [104] J. Carreira and A. Zisserman, “Quo vadis, action recognition? a new model and the kinetics dataset,” in *proceedings of the IEEE Conference on Computer Vision and Pattern Recognition*, 2017, pp. 6299–6308.
- [105] Z. Tu, H. Li, D. Zhang, J. Dauwels, B. Li, and J. Yuan, “Action-stage emphasized spatiotemporal vlad for video action recognition,” *IEEE Transactions on Image Processing*, vol. 28, no. 6, pp. 2799–2812, 2019.
- [106] H. Wang and C. Schmid, “Action recognition with improved trajectories,” in *Proceedings of the IEEE international conference on computer vision*, 2013, pp. 3551–3558.
- [107] L. Wang, Y. Xiong, Z. Wang, Y. Qiao, D. Lin, X. Tang, and L. V. Gool, “Temporal segment networks: Towards good practices for deep action recognition,” in *European conference on computer vision*. Springer, 2016, pp. 20–36.